Danicamtiv reduces myosin's working stroke but enhances contraction by activating the thin filament

Brent Scott[1], Lina Greenberg[1], Caterina Squarci[2], Kenneth S. Campbell[2], and Michael J. Greenberg[1,*]

[1]Department of Biochemistry and Molecular Biophysics, Washington University School of Medicine, St. Louis, MO, 63110, USA
[2] Division of Cardiovascular Medicine, University of Kentucky, Lexington, KY, 40506, USA

[*]Corresponding author:

Michael J. Greenberg
Department of Biochemistry and Molecular Biophysics
Washington University School of Medicine
660 S. Euclid Ave., Campus Box 8231
St. Louis, MO 63110
Phone: (314) 362-8670
Email: greenberg@wustl.edu

Keywords: single molecule, contractility, cardiac myosin

Running title: Danicamtiv's molecular effects

ABSTRACT

Heart failure is a leading cause of death worldwide, and even with current treatments, the 5-year transplant-free survival rate is only ~50-70%. As such, there is a need to develop new treatments for patients that improve survival and quality of life. Recently, there have been efforts to develop small molecules for heart failure that directly target components of the sarcomere, including cardiac myosin. One such molecule, danicamtiv, recently entered phase II clinical trials; however, its mechanism of action and direct effects on myosin's mechanics and kinetics are not well understood. Using optical trapping techniques, stopped flow transient kinetics, and *in vitro* reconstitution assays, we found that danicamtiv reduces the size of cardiac myosin's working stroke, and in contrast to studies in muscle fibers, we found that it does not affect actomyosin detachment kinetics at the level of individual crossbridges. We demonstrate that danicamtiv accelerates actomyosin association kinetics, leading to increased recruitment of myosin crossbridges and subsequent thin filament activation at physiologically-relevant calcium concentrations. Finally, we computationally model how the observed changes in mechanics and kinetics at the level of single crossbridges contribute to increased cardiac contraction and improved diastolic function compared to the related myotrope, omecamtiv mecarbil. Taken together, our results have important implications for the design of new sarcomeric-targeting compounds for heart failure.

44 **SIGNIFICANCE STATEMENT**

45 Heart failure is a leading cause of death worldwide, and there is a need to develop new
46 treatments that improve outcomes for patients. Recently, the myosin-binding small molecule
47 danicamtiv entered clinical trials for heart failure; however, its mechanism at the level of
48 single myosin crossbridges is not well understood. We determined the molecular
49 mechanism of danicamtiv and showed how drug-induced molecular changes can
50 mechanistically increase heart contraction. Moreover, we demonstrate fundamental
51 differences between danicamtiv and the related myosin-binding small molecule omecamtiv
52 mecarbil that explain the improved diastolic function seen with danicamtiv. Our results have
53 important implications for the design of new therapeutics for heart failure.

54 **INTRODUCTION**

55 Heart failure, a leading cause of mortality and morbidity in the world, is characterized
56 by the inability of the heart to generate sufficient power to perfuse the body at normal filling
57 pressures. Heart failure with reduced ejection fraction (HFrEF) is characterized by reduced
58 contractility during systole, and it accounts for ~50% of heart failure cases (1). Current
59 treatments for HFrEF (e.g., beta blockers and ACE inhibitors) target adverse remodeling of
60 the heart, which occurs secondary to reduced contractile function. While targeting adverse
61 remodeling has significantly improved outcomes for patients with HFrEF, the 5-year
62 transplant-free survival rates are still only ~50-70% (2). Thus, there is an outstanding need
63 to develop new therapeutics that improve mortality and quality of life for patients with HFrEF.

64 There has been a long-standing interest in developing heart failure treatments that
65 reverse the reduced contractile function seen in patients with HFrEF, but this approach has
66 been met with several challenges. Inotropes, such as milronone, increase heart contractility
67 by modulating calcium flux; however, elevated calcium leads to increased mortality (3), and
68 as such, inotropes are typically only used with patients in end-stage heart failure (1).
69 Recently, there have been several efforts to develop small molecules that directly target the
70 sarcomeric machinery to increase cardiac contraction without affecting calcium handling (4-
71 9). The first of these drugs was omecamtiv mecarbil (OM) (4), which was discovered in a
72 high-throughput screen for small molecules that increase cardiac myosin's ATPase activity.
73 OM made it to phase III clinical trials (10); however, the FDA declined to approve OM due to
74 its limited effect size and negative effects on relaxation.

75 Recently, a new myosin-binding compound was reported, danicamtiv, and this small
76 molecule is currently in phase II clinical trials for HFrEF (11). Currently, there is limited
77 information about the mechanism of danicamtiv, and the direct molecular effects of
78 danicamtiv on the kinetics and mechanics of individual myosin crossbridges is poorly
79 understood. In a study comparing OM and danicamtiv, it was reported that danicamtiv has

a smaller impact on relaxation compared to OM (9); however, the molecular mechanism underlying this difference is not known. Moreover, elegant experiments in muscle fibers and myofibrils have shown clear structural and functional effects of danicamtiv at the cellular and sub-cellular levels (12-14). X-ray diffraction of danicamtiv treated muscle fibers revealed an increase in filament lattice spacing and a re-positioning of myosin heads closer towards the thin filament (14). Moreover, danicamtiv was shown to slow the rate of tension development in porcine myofibrils (14), slow tension redevelopment in human myocardial bundles (13), slow the rate of myofibril relaxation (14), and slow the rate of myosin-driven motility *in vitro* (14). Based on these observations, it was suggested that danicamtiv likely slows the rate of ADP release from actomyosin, the transition that limits actomyosin dissociation in cycling muscle; however, the direct effects of danicamtiv at the level of single crossbridges has not been examined.

Here, we use a combination of stopped flow transient kinetics, single molecule optical trapping, computational modeling, and in vitro reconstitution assays to directly measure how danicamtiv affects the mechanics and kinetics of individual myosin crossbridges. Our results provide new insights into the mechanism of danicamtiv and help to explain its differences with OM.

100 **RESULTS**

101 We set out to measure the effects of danicamtiv on the mechanics and kinetics of
102 individual cardiac myosin crossbridges. We used porcine cardiac actin, which is identical to
103 the human isoform, and porcine ventricular cardiac myosin which has biophysical properties
104 that are indistinguishable from human cardiac myosin (15-17). Danicamtiv was dissolved in
105 DMSO (10 mM) and diluted in KMg25 Buffer to a final concentration of 10 μM for all
106 experiments. The final experiment buffers contained 0.1% DMSO. First, we examined the
107 effects of danicamtiv on myosin's steady-state ATPase activity. Similar to previous reports
108 using isolated myofibrils (11), we found that danicamtiv increases myosin's maximal steady-
109 state ATPase rate at saturating actin by ~1.2-fold (P = 0.028) and increases the effective K_m
110 (P = 0.01) (**Fig. 1A, Table 1**). Next, we used an *in vitro* motility assay in which fluorescently
111 labeled actin is translocated over a bed of myosin in the presence of ATP (18) and we
112 measured the speed of myosin-based movement. Consistent with previous reports, we
113 observed that danicamtiv reduces the motile speed by ~55% (**Fig. 1B**) (P = $4x10^{-6}$). Taken
114 together, danicamtiv accelerates the overall rate of myosin crossbridge cycling kinetics while
115 reducing the speed at which it moves actin.

116

117 **Danicamtiv does not affect key biochemical transitions that govern actomyosin**
118 **detachment (ADP release or ATP-induced dissociation)**

119 Our data demonstrate that danicamtiv increases overall cycling kinetics while
120 simultaneously reducing the speed of myosin motility, suggesting that danicamtiv affects the
121 coupling between the mechanics and kinetics of myosin crossbridges. In the motility assay,
122 the speed of actin filament translocation is proportional to the displacement generated by a
123 single myosin (i.e., the size of the myosin working stroke) divided by the amount of time that
124 myosin remains attached to the actin filament (19):

125 $$\text{speed} \propto \text{displacement} / \text{attachment time} \qquad \text{Eq. 1}$$

126 Thus, the ~50% reduction in motile speed suggests that either the displacement generated
127 by the myosin is reduced by half or the attachment time of a crossbridge gets twice as long.
128 Therefore, we set out to directly test these two possibilities.

129 To test whether danicamtiv affects the time that crossbridges remain bound to actin,
130 we measured the rates of key biochemical transitions. The amount of time that actin and
131 myosin remain attached is set by the time required for ADP release and subsequent ATP-
132 induced actomyosin dissociation (20). Since the rate of a transition is inversely proportional
133 to the average time for the transition to occur, we can equivalently state that the rate of
134 crossbridge dissociation is set by the rates of ADP release from myosin and ATP-induced
135 dissociation of actomyosin (**Fig. 1C**). Therefore, we measured the rates of these transitions
136 using stopped flow transient kinetics.

137 First, we measured the rate of ATP-induced actomyosin dissociation using pyrene-
138 labeled actin as a fluorescent reporter of actomyosin binding (21), where myosin detachment
139 from pyrene-labeled actin causes an increase in pyrene fluorescence. We rapidly mixed
140 pyrene-labeled actomyosin with a range of ATP concentrations and measured the change
141 in fluorescence. As previously described, fluorescence transients were well fitted by the
142 sum of two exponential functions, where the observed rate of the fast phase can be used to
143 report the rate of ATP-induced actomyosin dissociation (21). The relationship between the
144 observed rate of the fast phase and the concentration of ATP was fitted with a hyperbolic
145 function to obtain the maximal rate of ATP-induced dissociation at saturating ATP
146 concentrations, k_{+2}', and the concentration of ATP necessary to reach half-maximal
147 saturation, $1/K_1$' (**Fig. 2A**). We found that danicamtiv does not affect the maximal rate of
148 ATP-induced dissociation (P = 0.99), the concentration of ATP necessary to reach half-
149 maximal saturation (P = 0.64), or the second-order rate of ATP induced dissociation (4.0 ±
150 0.7 vs 4.4 ± 1.1 $\mu M^{-1}s^{-1}$, for 0 and 10 μM danicamtiv, P = 0.64) (**Table 1**). Thus, changes in

151 ATP-induced actomyosin dissociation cannot explain the reduced motility seen with
152 danicamtiv.

153 Next, we measured the rate of ADP release from actomyosin by preparing a mixture
154 of ADP-saturated myosin and pyrene-labeled actin, and rapidly mixing this with saturating
155 amounts of ATP, leading to an increase in fluorescence (21). The fluorescence transients
156 were fitted with single exponential functions to obtain the rate of ADP release from
157 actomyosin (**Fig. 2B**). We found that the rates of ADP release with and without 10 μM
158 danicamtiv were not statistically different (WT: 73 ± 3 s^{-1}, Danicamtiv: 73 ± 3 s^{-1}, P = 0.96).
159 This rate of ADP release is consistent with previous measurements using porcine β-cardiac
160 myosin (16, 22) and recombinant human cardiac myosin (23). Moreover, at physiologically
161 relevant saturating ATP concentrations, the rate of ADP release is slower than the rate of
162 ATP-induced actomyosin dissociation both in the presence and absence of danicamtiv. As
163 such, the rate of ADP release limits actomyosin dissociation at saturating ATP
164 concentrations, such as those in the motility assay and in cardiomyocytes. Taken together,
165 the observed reduction in motile speed cannot be explained by changes in the rate of ADP
166 release from actomyosin.

167 It has also been proposed that danicamtiv might affect the rate of ADP binding to
168 actomyosin (14). To test this, we determined the ADP binding affinity to actomyosin by
169 measuring the rate of pyrene-actomyosin dissociation in the presence of competing mixtures
170 of ATP and ADP (21). We found that the ADP affinity was not statistically different with or
171 without danicamtiv (**Fig. 2C**; P = 0.87). Moreover, we can use this affinity and the measured
172 ADP release rate to calculate the rate of ADP binding (k_{-5}' see Methods for details), and we
173 found that there is no statistical difference in the rate of ADP rebinding with danicamtiv (P =
174 0.4). Taken together, we did not observe changes in the rates of key steps of actomyosin
175 dissociation that could explain the reduction in motile speed.

176 Finally, we measured the rate of ATP hydrolysis by myosin at saturating ATP
177 concentrations using the intrinsic tryptophan fluorescence of the myosin that increases with
178 hydrolysis (**Fig. 2D**) (21). We found that the observed fluorescence transients are well fitted
179 by a single exponential function. We observe that the rate of hydrolysis (k_3 *(obs)*, **Table 1**)
180 is 70 s^{-1}, consistent with previous reports (23), and this rate is not significantly different in
181 the presence or absence of danicamtiv (P = 0.42).
182

183 **Danicamtiv reduces the displacement of myosin's working stroke without altering**
184 **detachment kinetics**

185 Given that we did not observe a change in biochemical kinetics that could explain the
186 ~50% reduction in motile speed with danicamtiv (**Fig. 1B**), we used single molecule optical
187 trapping techniques to measure the mechanics of the cardiac myosin working stroke in the
188 presence and absence of danicamtiv (16, 24). We used the three-bead assay in which an
189 actin filament is suspended between two optically-trapped beads and lowered onto a
190 surface-bound pedestal that is sparsely coated with myosin (25) (**Fig. 3A**). We were able
191 to clearly resolve single molecule interactions between actin and myosin (**Fig. 3B**), enabling
192 us to probe the mechanics and kinetics of the myosin working stroke.

193 First, we measured single molecule interactions between actin and myosin at low,
194 non-physiological ATP concentrations (10 μM ATP) to facilitate the observation of substeps
195 of the myosin working stroke. The size of the working stroke can be measured by fitting
196 single exponential functions to the time forward ensemble averages (**Fig. 3C**) or by
197 calculating the relative position change that occurs with each actomyosin interaction (**Fig.**
198 **3D**). Both analyses provide similar results (**Table 2**). We found that in the absence of
199 danicamtiv, cardiac myosin has a working stroke size of 5.0 nm, consistent with previous
200 measurements of human and porcine cardiac myosins (15-17, 26). We found that in the
201 presence of danicamtiv, the total size of myosin's working stroke was reduced to 2.5 nm (P

202 < 0.01; **Fig. 3C**). This ~50% reduction in the working stroke displacement is consistent with
203 the 55% decrease in speed we observed in motility (**Fig. 1B**).

204 Optical trapping also enables the direct measurement of the actomyosin attachment
205 duration. Cumulative distributions of attachment durations were generated and fitted with a
206 single exponential function to obtain the rate of actomyosin detachment (**Fig. 3E**). We found
207 that the detachment rate in the absence of danicamtiv at 10 μM ATP was 23 (-2.5/+2.5) s^{-1},
208 consistent with the expected rate of detachment based on the stopped flow measurements
209 (**Fig. 2**). Moreover, we found that there was no statistically significant difference in the
210 actomyosin detachment rate in the presence of danicamtiv at 10 μM ATP compared to the
211 DMSO control (24 (-0.8/+0.9) s^{-1}, P = 0.39, **Fig. 3E**), consistent with our stopped flow
212 measurements which suggested that danicamtiv does not change actomyosin detachment
213 kinetics. This result contrasts with OM. Consistent with previous studies, we show that OM
214 further reduces the size of the working stroke compared to danicamtiv and significantly slows
215 the rate of actomyosin dissociation in the optical trap (**Supp. Fig. 1**) (15). Taken together,
216 our results suggest that unlike OM, danicamtiv does not affect the kinetics of actomyosin
217 detachment at the single molecule level at low ATP.

218 To ensure that our observations in the optical trap at 10 μM ATP were not a result of
219 working at low ATP concentrations, we also collected an additional optical trapping dataset
220 at a physiologically-relevant saturating ATP concentration (1 mM) (**Supp. Fig. 2**). At 1 mM
221 ATP we observed that myosin's displacement is reduced ~50% with danicamtiv (P < 0.01).
222 Moreover, we do not observe a difference in the actomyosin detachment rate with danicamtiv
223 (P = 0.15, **Table 2**), consistent with our observations at low ATP and the stopped flow
224 measurements.

225 Next, we tested whether danicamtiv affects myosin's load-dependent detachment
226 kinetics at the level of single molecules at 1 mM ATP (**Fig. 4A**). To do this, we used a
227 feedback loop to exert force on the myosin during its working stroke, and we measured the

228 actomyosin attachment duration under load (16). The relationship between force and
229 attachment duration can be fit to extract the rate of the primary force-sensitive transition in
230 the absence of force, k_0, and the distance to the transition state (a measure of force
231 sensitivity) (**Fig. 4B**) (27). We found that at saturating ATP concentrations, the rate of the
232 primary force sensitive transition in the absence of danicamtiv was 61 (-21/+40) s^{-1},
233 consistent with the rate of ADP release measured in the stopped flow (**Fig. 2B**) and previous
234 measurements (16, 26), and this rate was not statistically different in the presence of
235 danicamtiv (89 (-18/+24) s^{-1}, P = 0.12). Moreover, the distance to the transition state was
236 not statistically different in the absence or presence of danicamtiv (d = 1.4 (-0.37/+0.46) nm
237 vs 1.25 (0-.16/+0.17) nm, respectively, P = 0.35). Thus, danicamtiv does not change the
238 load-dependent kinetics of cardiac myosin at physiologically-relevant ATP concentrations,
239 and the observed reduction in motile speed (**Fig. 1B**) can be explained by a reduction in the
240 size of the myosin working stroke (**Fig. 3C**).
241
242 **Danicamtiv increases the kinetics of actomyosin attachment**
243 Our results clearly demonstrate that at the level of single crossbridges, danicamtiv
244 does not affect actomyosin detachment kinetics. Therefore, we investigated whether
245 danicamtiv affects actomyosin attachment kinetics. Our steady-state ATPase
246 measurements (**Fig. 1A**) demonstrate that danicamtiv increases the overall steady-state
247 ATPase rate, indicative of the fact that danicamtiv increases the rate of the slowest step of
248 the ATPase cycle. For β-cardiac myosin cycling in the presence of actin, the overall cycle
249 rate is limited by attachment kinetics (23). Since danicamtiv increases the steady state
250 ATPase without altering detachment kinetics, we posited the increase in ATPase could be a
251 result of danicamtiv accelerating attachment kinetics.
252 To test whether danicamtiv affects attachment kinetics, we used stopped flow
253 techniques to measure the rates of actomyosin attachment and detachment under single

254 turnover conditions (28) (**Fig. 5A,** see Supplemental Materials for additional details). Myosin
255 was preincubated with an excess of pyrene-labeled actin to form a rigor complex that
256 quenches pyrene's fluorescence. The actomyosin was then rapidly mixed with a sub-
257 saturating concentration of ATP, causing an increase in fluorescence that reports the
258 actomyosin detachment rate at this ATP concentration, k_{det}. A low concentration of ATP is
259 used to ensure that this process only occurs once (i.e., a single turnover). Once off actin,
260 myosin hydrolyzes ATP and then re-attaches to actin, quenching the pyrene fluorescence
261 and reporting the rate of myosin attachment at this actin concentration, k_{att}.

262 The single turnover fluorescence transients consisted of two phases, where the rate
263 of detachment was faster than the rate of attachment, consistent with the notion that the rate
264 of attachment limits the overall ATPase cycle time (**Fig. 5B, Supp. Figs. 3 and 4**). We saw
265 that there was no statistically significant difference in the rate of detachment in DMSO or
266 danicamtiv. (3.8 ± 0.9 vs 4.2 ± 0.8 s^{-1}, respectively, P = 0.23, **Fig. 5C**). This measured
267 detachment rate is in agreement with the second-order rate of ATP-induced dissociation at
268 0.75 μM ATP measured in the stopped flow (**Table 1**). We also saw that the observed
269 attachment rate was significantly faster with 10 μM compared to DMSO controls (0.0040 ±
270 0.0002 vs 0.0063 ± 0.0006 $\mu M^{-1} \cdot s^{-1}$, respectively, P < 0.001, **Fig. 5D**). Taken together, our
271 data demonstrate that danicamtiv increases attachment kinetics without affecting
272 detachment kinetics.

273

274 **Danicamtiv-induced increase in the myosin attachment rate causes increased thin**
275 **filament activation**

276 Given that danicamtiv increases the attachment rate of myosin to actin, we
277 hypothesized that this would lead to an increase in the fraction of myosin heads bound to
278 actin (i.e., the duty ratio). To test this hypothesis, we used a well-established variation of the
279 *in vitro* motility assay where the speed of actin filament movement was measured as a

280 function of surface myosin (29, 30). Actin filaments move at their maximal speed if there is
281 a sufficient concentration of myosin on the surface to ensure that at least one myosin head
282 is attached to the filament at any given time. We observed that despite moving slower,
283 danicamtiv-treated myosin required less myosin to reach saturation, consistent with an
284 increased duty ratio with drug (**Figs. 6A and B**).

285 Given the increase in the rate of myosin binding to actin with danicamtiv, we
286 hypothesized that danicamtiv would increase myosin-induced thin filament activation, since
287 thin filament activation depends on myosin binding (31). To test this, we reconstituted thin-
288 filaments in the *in vitro* motility assay, and we measured the speed of myosin-based
289 translocation over a range of calcium concentrations. We saw that danicamtiv increased thin
290 filament motility at submaximal calcium levels where the motility speed is limited by the rate
291 of myosin attachment (e.g. at pCa 7, 16 ± 28 vs. 51 ± 31 nm/s, $P < 0.001$) (**Fig. 6C**). These
292 low calcium levels are within the physiological range of calcium concentrations seen in
293 muscle (32). Taken together, our data suggest that danicamtiv-induced increases in
294 attachment kinetics lead to increased thin filament activation at submaximal calcium
295 concentrations.

296

297 **Computational modeling connects molecular effects and muscle function**

298 To better understand how changes at the molecular scale with danicamtiv would
299 translate into altered muscle contraction, we used computational modeling. We used a
300 spatially explicit model of muscle contraction, FiberSim (33). This model has previously
301 been used to successfully model several physiologically important parameters, including the
302 force-calcium relationship and the force generated in response to a calcium transient.

303 We used FiberSim to model the effects of danicamtiv on key muscle parameters
304 based on our molecular measurements. Our results show that danicamtiv reduces the size
305 of the working stroke while increasing the rate of crossbridge attachment. Moreover,

306 previous X-ray diffraction studies have shown that danicamtiv causes myosin to transition
307 from an autoinhibited interacting heads motif to an activated disordered relaxed state (14).
308 We adjusted the model input parameters to match these changes, and we simulated the
309 effects of each of these changes in isolation (**Supp. Fig. 5**) and all together (**Figs. 6E and**
310 **F**). We simulated both the force-calcium relationship and the force generated in response to
311 a calcium transient. When looking at the composite effects of all three changes, we see that
312 this causes a shift in the force calcium relationship towards submaximal calcium activation
313 (**Fig. 6E**) that agrees well with our experimental measurements (**Fig. 6D**). Moreover, the
314 modeling shows that danicamtiv is expected to increase both the magnitude of the force
315 generated in response to a calcium transient with slight slowing of both the rates of force
316 development and relaxation (**Fig. 6F**). Finally, the modeling predicts that danicamtiv will
317 increase the force-time integral (**Fig. 6G**). Taken together, our modeling provides insights
318 into how danicamtiv affects the kinetics and mechanics of myosin, leading to increased
319 muscle function.

320 **DISCUSSION**

321

322 **At the level of single crossbridges, danicamtiv's biophysical mechanism is more**
323 **complicated than a "myosin activator"**

324 Our observation of ~50% reduced motility with danicamtiv (**Fig. 1B**) is consistent with
325 the excellent study by Kooiker et al. (14). Previously, it was suggested that this reduced
326 speed could be due to danicamtiv's effects on ADP binding and release, since the rate of
327 ADP release limits the shortening speed of muscle (34). We directly measured the rate of
328 ADP binding, rate of ADP release, and the equilibrium constant for ADP binding, and we do
329 not see changes in any of these parameters (**Figs. 2B and C**). Moreover, we directly
330 measured the rate of actomyosin dissociation in the optical trap at both high and low ATP
331 concentrations, and we did not observe any changes in the detachment rate (**Fig. 3E**). We
332 also measured the load-dependent detachment kinetics in the optical trap, and we did not
333 observe any changes with danicamtiv treatment (**Fig. 4**). Finally, we used a single turnover
334 stopped flow assay, and we do not see any difference in the detachment kinetics (**Fig. 5C)**
335 Taken together, our results demonstrate that danicamtiv does not have effects on the rate
336 of ADP release or actomyosin detachment at the level of single crossbridges.

337 The speed in the motility assay is proportional to the step size of the myosin divided
338 by the amount of time that the crossbridge remains attached (19). While we did not observe
339 any changes in attachment time in the optical trap, we did observe a ~50% decrease in the
340 size of the myosin working stroke (**Fig. 3E**). As such, the ~50% decrease in motility speed
341 can be explained by a ~50% reduction in the size of the working stroke. Taken together, at
342 the level of individual crossbridges, the reduced speed in motility seen with danicamtiv
343 cannot be explained by changes in detachment kinetics, rather, it is due to a decrease in the
344 size of the myosin working stroke.

345 Danicamtiv was initially discovered in a high-throughput screen for molecules that
346 activate the steady-state ATPase activity of myosin, and as such, it was initially classified as
347 a myosin activator (11); however, as we show here, it has a more complex biophysical
348 mechanism at the level of single crossbridges. The ATPase assay uses a minimal number
349 of components (i.e., myosin, actin, and ATP) to measure the steady-state rate of ATP
350 turnover. While this assay is useful for drug screening due to its well-characterized and
351 easily measured outputs, it also has important limitations due to its simplified nature. This
352 assay considers only the effects of drugs on kinetics, and it does not consider effects on
353 mechanics or incorporate higher-order structures that are important for muscle function
354 (e.g., sarcomere lattice, myosin autoinhibition in the thick filament, calcium-based
355 regulation). This limitation becomes clear in the case of danicamtiv, where mechanics and
356 kinetics are uncoupled. We show that danicamtiv is an activator of myosin's steady-state
357 ATPase rate (**Fig. 1A**), but an inhibitor of myosin mechanics (**Fig. 3C**). This demonstrates
358 that danicamtiv partially uncouples myosin mechanics and kinetics, and its biophysical
359 mechanism is more complicated than a simple myosin activator. We propose that
360 danicamtiv should be classified as a myosin-binding sarcomeric activator.
361

362 **Danicamtiv's activating properties emerge in higher-order structures**

363 Since danicamtiv has both inhibitory and activating effects at the level of individual
364 crossbridges, we further investigated its effects in higher-order structures. Increased
365 cardiac contractility has been observed in muscle fibers, small animal models, and humans
366 (9, 11-14, 35). One difference between actomyosin in isolation and in muscle is the
367 presence of the thin filament regulatory proteins, tropomyosin and troponin. In the absence
368 of calcium, tropomyosin blocks the myosin strong binding sites on actin, preventing myosin
369 attachment and subsequent force generation (36). During systole, calcium binds to troponin,
370 leading to movement of tropomyosin followed by attachment of myosin crossbridges. Thus,

371 the process of thin filament activation depends both on both calcium and myosin binding to
372 the thin filament.

373 Here, we observed that danicamtiv increases the rate of myosin attachment to actin
374 (**Figs. 1A and 5D**). As such, we hypothesized that increased attachment would lead to
375 increased binding to the thin filament, causing activation of the thin filament at submaximal
376 calcium levels. In fact, this is what we observe in the *in vitro* motility assay using regulated
377 thin filaments, and similar shifts were seen in muscle fiber experiments (12-14). To test
378 whether this increased myosin attachment could contribute to the observed changes in
379 muscle fiber force, we performed computational modeling of the sarcomere using FiberSim
380 (**Fig. 6E**). We found that changing myosin's rate of attachment to the thin filament alone is
381 sufficient to recapitulate the shift towards submaximal calcium activation that we observed
382 in the *in vitro* motility assay (**Supp. Fig. 5**). Taken together, we propose that danicamtiv
383 increases muscle contraction, in part, through activation of the thin filament.

384 As mentioned above, simplified systems cannot capture all aspects of cardiac
385 contraction, and previous studies in muscle fibers have demonstrated several effects that
386 we cannot observe at the level of individual crossbridges (12-14). To gain some insights
387 into how changes at the level of individual crossbridges translates into muscle function, we
388 used a spatially explicit model of muscle contraction to simulate key physiological
389 parameters (**Figs. 6E and F** and **Supp. Fig. 5**). We simulated the individual and composite
390 effects of (1) increased crossbridge attachment based on **Figs. 1A** and **5D**, (2) decreased
391 working stroke size based on **Figs. 1B** and **3C**, and (3) an increase in the number of myosin
392 crossbridges available to interact with the thin filament based on X-ray diffraction studies of
393 muscle fibers (14). Our results clearly demonstrate that these danicamtiv-induced changes
394 at the level of single crossbridges are sufficient to reproduce the shift towards submaximal
395 calcium activation, increased peak force production in response to a calcium transient, and
396 an increase in the force-time integral. Moreover, we observe slightly slowed rates of force

397 development and relaxation with danicamtiv that emerge without changes in the rate of
398 crossbridge detachment. Taken together, our results demonstrate the importance of
399 multiscale studies for understanding the mechanisms of small molecules targeting myosin.
400

401 **Comparison with omecamtiv mecarbil**

402 The first compound targeting cardiac myosin for the treatment of systolic heart failure
403 was omecamtiv mecarbil (OM) (5, 6). Like danicamtiv, OM was also identified in a screen
404 for small molecules that increase myosin's steady-state ATPase activity. OM made it to
405 stage III clinical trials, but ultimately the FDA declined to approve OM due to its limited effect
406 size and its impact on cardiac relaxation (10). In particular, patients treated with OM showed
407 prolonged systole and impaired relaxation, which lead to an increase in serum troponin,
408 indicative of cardiac damage.

409 There are some similarities between OM and danicamtiv seen at the molecular scale.
410 Both danicamtiv and omecamtiv increase myosin's ATPase activity and slow the rate of
411 motility (5, 37). Both danicamtiv and OM decrease the size of the myosin working stroke
412 (15); however, the reduction in the size of the working stroke with danicamtiv was not as
413 severe as the reduction caused by OM (**Supp. Fig. 1C**). The decrease in size of the working
414 stroke can be seen for both OM and danicamtiv; however, this effect is more pronounced
415 for OM which almost completely eliminates the working stroke.

416 The key difference between OM and danicamtiv is that omecamtiv significantly
417 increases the amount of time that actin and myosin remain attached while danicamtiv does
418 not. This can be seen in **Supp. Fig 1D**. This subtle difference has important implications for
419 the mechanism of action. OM increases the attachment duration, leading to slowed
420 detachment of myosins, prolonging systole. This effect would not be expected for
421 danicamtiv, suggesting that it might have better effects on relaxation and diastolic function.
422 Consistent with this notion, experiments using engineered heart tissues and muscle fibers

423 showed that danicamtiv has a lower impact on relaxation than OM (9, 13). It is worth noting
424 however, that while the effects of danicamtiv on diastolic function are smaller that OM, they
425 still exist (9, 35), and we can observe evidence of slowed relaxation in our computational
426 modeling. It remains a challenge to the field to develop small molecules that can uncouple
427 myosin's effects on systole and diastole.
428

429 **Conclusions**

430 Here, we demonstrate the effects of danicamtiv on single crossbridges and highlight
431 how properties at the single molecule level translate into effects seen in muscle fibers.
432 Importantly, our results demonstrate that danicamtiv is a myosin binding sarcomeric
433 activator that exerts its effects in part through thin filament activation.

Acknowledgements:

The authors acknowledge financial support provided by the National Institutes of Health (R01 HL141086 to M.J.G., R01 HL148785 to K.S.C., T32 HL125241 to B.S.), the Children's Discovery Institute of Washington University and St. Louis Children's Hospital (PM-LI-2019-829 M.J.G.), and the American Heart Association (TPA 970198 to M.J.G).

Conflict of interest statement:

All experiments were conducted in the absence of any commercial or financial relationships that could be construed as potential conflicts of interest. M.J.G. discloses research funding from Edgewise Therapeutics on an unrelated project.

Author contributions:

Conception and oversight by M.J.G.. ATPase experiments were conducted by L.G.. Computational modeling was conducted by C.S., K.S.C., and B.S.. All single molecule and transient kinetic experiments were conducted by B.S.. All authors contributed to the analysis of the data. The first draft was written by M.J.G.. All authors contributed to the writing and/or editing of the manuscript.

451 **MATERIALS AND METHODS**

452

453 Full experimental procedures can be found in the Supplemental Materials.

454

455 **Biochemical Kinetic Measurements**

456 Porcine ventricular actin and myosin were purified from tissue, and human troponin and
457 tropomyosin were recombinantly expressed in *E. coli* (22). Actin was labeled with pyrene
458 as previously described (22). Danicamtiv was purchased from Selleckchem (99.1% purity,
459 S9948). ATPase measurements as a function of actin concentration were conducted using
460 the NADH enzyme coupled assay (21, 38). Stopped flow measurements were conducted
461 in an SX-20 instrument (Applied Photophysics). Using these techniques, we measured the
462 rates of ATP induced actomyosin dissociation, ADP release, ADP hydrolysis, ADP binding
463 affinity, and single turnover kinetics (21).

464

465 ***In Vitro* Motility and Optical Trapping Experiments**

466 *In vitro* motility assays were conducted as previously described, where actin filaments
467 translocate over a bed of myosin in the presence of ATP (39, 40). Thin filament regulation
468 was reconstituted by adding calcium and the regulatory proteins troponin and tropomyosin.
469 Optical trapping was done using the three-bead assay in which an actin filament is stretched
470 between two optically trapped beads and lowered on to a pedestal bead that is sparsely
471 coated with myosin (16, 24, 27). Data were analyzed using the SPASM software (24).

472

473 **Computational modeling**

474 Computational modeling was done using FiberSim, a spatially explicit model of muscle
475 contraction (33). Model input parameters were modified to match experimental

measurements. The force-calcium relationship and the time-dependent response to a calcium transient were simulated.

Data Availability and Reproducibility

All data is included in the project repository hosted on Zenodo (10.5281/zenodo.12636349). All analysis was performed in R version 4.4.0 (R Core Team) unless otherwise noted. The code has been made available to reproduce verbatim all figures and related analyses in the project repository.

484 **Figure Legends**

485

486 **Figure 1. Steady state properties of β-cardiac myosin treated with danicamtiv. A)** The
487 steady-state myosin ATPase rate was measured using the NADH coupled assay. The
488 steady state myosin ATPase rate is plotted verses a function of actin concentration. Data
489 were fitted by a hyperbolic function to calculate the maximal cycling rate (V_{max}) and actin
490 affinity (K_m) with the Michaelis Menten equation. Treatment with 10 μM danicamtiv increased
491 the maximal rate by ~1.2 fold from 5.9 to 7.0 s^{-1} (P = 0.028) and decreased the K_m from 14.0
492 to 8.1 μM (P = 0.01). Each point represents the average rate from four independent trials
493 with error bars showing the standard deviation. Statistical testing done using a 2-tailed T-
494 test. Black = DMSO control. Pink = 10 μM danicamtiv. **B)** Speed of actin translocation in the
495 unregulated in vitro motility assay. The addition of 10 μM danicamtiv decreased motility
496 speed ~55% (P = $4x10^{-6}$). Thick horizontal lines show the average speed with standard
497 deviation shown by the thin horizontal lines. Points represent the average speed of all
498 filaments in a field of view for a single technical replicate measured across N = 3
499 independent experiments. Statistical testing done using a 2-tailed T-test. **C)** Scheme of
500 myosin's mechanochemical cross-bridge cycle. Myosin's rate limiting step is actin
501 attachment, so the predominant population of motors reside in the pre-working stroke
502 M.ADP.Pi state during steady state cycling. The steady-state ATPase is thus limited by actin
503 attachment (k_{att}) which is rapidly followed by the mechanical working stroke and phosphate
504 release. *In vitro* motility speed is limited by the ADP release rate (k_{+5}').

505

506 **Figure 2. Stopped-flow kinetics measured with and without 10 μM danicamtiv.** Black
507 = DMSO control. Pink = 10 μM danicamtiv. **A)** The rates of ATP-induced actomyosin
508 dissociation were measured in the stopped flow. Transients were well fitted by the sum of
509 two exponential functions, where the observed rate of the fast phase (k_{fast}) is plotted as a

510 function of ATP concentration. Data were fitted with a hyperbolic function to obtain K_1' and
511 k_{+2}'. There are no differences in either K_1' or k_{+2}' with or without danicamtiv (P = 0.64 and P
512 = 0.99, respectively). Each point represents an independent measurement over 3
513 experimental days. **B)** The rate of ADP release from actomyosin was measured using
514 stopped flow techniques, and the fluorescence transients were fitted with single exponential
515 functions. Note, both 0 and 10 μM danicamtiv are plotted and overlay. There is no statistically
516 significant difference in the rate of ADP release the absence or presence of danicamtiv (P =
517 0.96). **C)** The overall ADP binding affinity to actomyosin was measured by mixing an
518 actomyosin solution containing increasing concentrations of ADP with 50 μM ATP
519 (concentrations after mixing) measured using a competition experiment. The observed rate
520 as a function of ADP concentration was fitted with a hyperbolic function to determine the
521 ADP affinity (see methods). Each point shows the average of 3 separate trials and error bars
522 show the standard deviations. There is no difference in the ADP binding affinity (k_{-5}'; P =
523 0.40). **D)** The rate of ATP hydrolysis by myosin was measured using stopped flow
524 techniques. The rate of hydrolysis is reported by the change in tryptophan fluorescence at
525 saturating ATP concentrations. Fluorescence transients are well fitted with single
526 exponential functions. The observed rate of ATP hydrolysis (k_3 *(obs)*) was not different with
527 10 μM danicamtiv (P = 0.42). For all stopped-flow values, see **Table 1**.
528
529 **Figure 3. Single molecule optical trapping reveals that danicamtiv reduces the size of**
530 **myosin's working stroke without altering detachment kinetics.** Black = DMSO control.
531 Pink = 10 μM danicamtiv. **A)** Cartoon schematic of the optical trapping assay. An actin
532 filament is strung between two optically-trapped beads and lowered onto a pedestal bead
533 sparsely bound with myosin. **B)** Optical trapping data traces showing the stochastic binding
534 of myosin to actin. Binding interactions are shown in grey or pink and detached states are
535 shown in black. **C)** Time forward ensemble averages of myosin's working stroke reveal a

536 ~50% reduction in the size of myosin's total working stroke in the presence of danicamtiv.
537 **D)** The cumulative distribution of the total working stroke displacements at 10 μM ATP is well
538 fit by a single cumulative Gaussian function (dotted lines) with average values of 4.9 ± 9.7
539 nm versus 3.0 ± 9.0 nm for DMSO control and 10 μM danicamtiv, respectively ($P < 0.001$
540 using a two-tailed T-test). N = 2076 binding interactions for control and 4776 binding events
541 for 10 μM danicamtiv. **E)** The cumulative distributions of attachment durations at 10 μM ATP.
542 Single exponential functions were fit to the distributions using maximum likelihood
543 estimation. 95% confidence intervals were calculated using bootstrapping methods. There
544 is no statistical difference between control and 10 μM danicamtiv, 23 (-2.5/+2.5) s^{-1} vs. 24 (-
545 0.8/+0.9) s^{-1} ($P = 0.48$). For all trapping values, see **Table 2**.
546
547 **Figure 4. Danicamtiv does not alter myosin's load-dependent detachment kinetics at**
548 **1 mM ATP.** Black = DMSO control. Pink = 10 μM danicamtiv. **A)** An isometric force clamp
549 was used to maintain actin at an isometric position during myosin binding interactions. To
550 do this, the motor bead (M) was moved to hold the transducer bead (T) at an isometric
551 position. Data traces are shown. **B)** Plots of actomyosin attachment duration versus the
552 average resistive force applied during the binding event. Data are exponentially distributed
553 at each force. Each point represents an independent actomyosin binding interaction. The
554 data were fitted with the Bell equation using maximum likelihood estimation and 95%
555 confidence intervals were calculated for each parameter by bootstrapping. The detachment
556 rate in the absence of load, k_0, was not different between control and 10 μM danicamtiv, 61
557 (-21/+40) vs 89 (-18/+24) s^{-1} ($P = 0.17$). These values are consistent with our measurements
558 of the rates of ADP release from stopped-flow experiments. The distance to the transition
559 state, *d*, which measures the load-sensitivity of the detachment rate, was not different
560 between control and 10 μM danicamtiv, 1.40(-0.37/+0.46) vs 1.25 (-0.16/+0.17) nm ($P =$
561 0.43).

562

563 **Figure 5. Danicamtiv increases myosin's attachment rate in a single turnover stopped**
564 **flow assay.** Black = DMSO control. Pink = 10 μM danicamtiv. **A)** Schematic conceptually
565 describing the single turnover assay used to measure myosin's attachment and detachment
566 rates. In this assay, myosin and pyrene labeled actin are pre-incubated and then mixed with
567 a sub-saturating concentration of ATP. The pyrene fluorescence increases as myosins
568 detach from actin, and the increase in fluorescence reports the rate of detachment of myosin
569 from actin (k_{det}). Myosin then reattaches to actin, quenching the fluorescence and reporting
570 the attachment rate (k_{att}). **B)** Fluorescence transients from the single turnover assay. Data
571 were fitted as described in the Supplemental Methods. **C)** The average second-order rate
572 of detachment (k_{det}) was similar with and without 10 μM danicamtiv (3.8 ± 0.9 vs. 4.2 ± 0.8
573 s^{-1}; P = 0.23). **D)** The second-order rate of attachment (k_{att}) increased with the addition of 10
574 μM danicamtiv (0.0040 ± 0.0002 vs 0.0063 ± 0.0007 $\mu M^{-1} \cdot s^{-1}$; P = < 0.001). For **C** and **D**, the
575 thick lines show the average values, and the error bars show the standard deviation. The
576 individual points are the fitted second-order rates to individual transients collected across
577 three experimental replicates. Statistical testing was done using a two-tailed T-test after
578 passing a normality test.

579

580 **Figure 6. Danicamtiv increases motility speed in the presence of regulatory proteins**
581 **and these effects on muscle contraction can be recapitulated computationally.** Black
582 = DMSO control. Pink = 10 μM danicamtiv. **A and B)** Unregulated *in vitro* motility speed as
583 a function of the myosin concentration on the flowcell surface. The speed decreases if there
584 is not at least one active myosin head bound to actin at any given time. Thus, if the duty
585 ratio increases with drug, less myosin will be required to reach saturation. 10 μM danicamtiv
586 decreases motility speed at higher myosin concentrations but increases speed at low myosin
587 concentrations, indicative of a higher duty ratio, despite having a smaller working stroke. **A)**

588 shows the measured speed and **B)** shows normalized data. ~40 filaments were tracked
589 across four fields of view from two different experimental preparations. **C and D)** Regulated
590 i*n vitro* motility speed using thin filaments decorated with troponin and tropomyosin as a
591 function of calcium. The data were fitted with the Hill equation and the fitted values ±
592 standard error are: V_{max} values are 386 ± 8 vs. 135 ± 7 nm/s ($P < 0.001$), pCa50 values are
593 5.76 ± 0.02 vs. 6.1 ± 0.09 ($P = 0.01$), and the Hill coefficients are 3.4 ± 0.4 vs 3.1 ± 1.5 ($P =$
594 0.85) for the control vs. 10 μM danicamtiv, respectively **C)** Shows the measured speed and
595 **D)** shows the data normalized to the fitted V_{max} and V_{min}. Each point represents average
596 speed with error bars showing the standard deviation of ~40-60 filaments imaged from 4-6
597 fields of view from 2-3 experimental replicates. **E)** Simulated force-calcium relationship from
598 FiberSim. To simulate danicamtiv, we incorporated increased actin attachment, reduced
599 myosin working stroke, and an increase in the population of active myosin heads.
600 Simulations recapitulate the shift seen in the motility experiments. **F)** Simulated twitch in
601 response to a calcium transient using the same simulation parameters. Danicamtiv
602 increases the maximal force, slows kinetics, and **G)** increases the force-time integral.

603 **FIGURES**

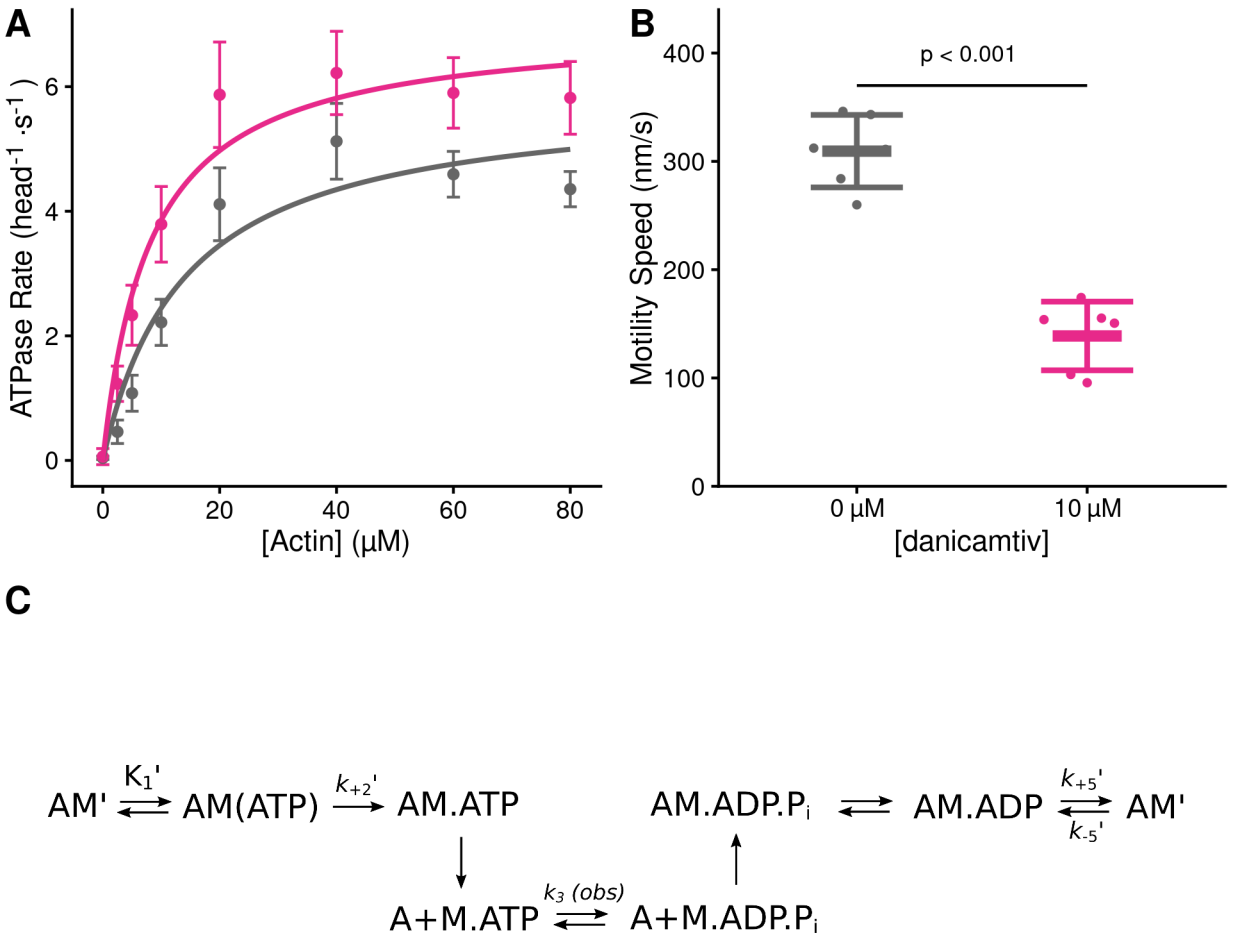

604

605 **Figure 1**

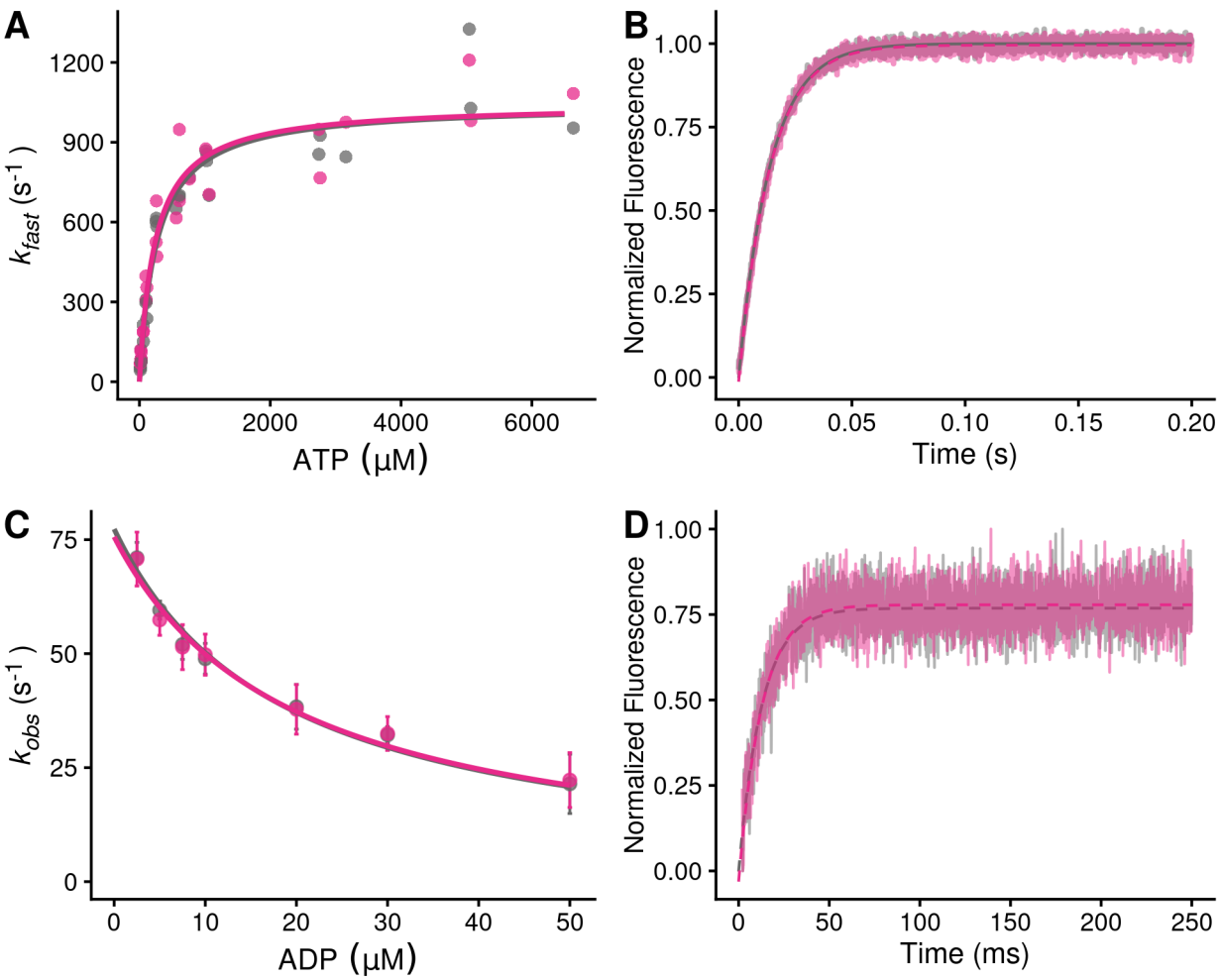

606

607 **Figure 2**

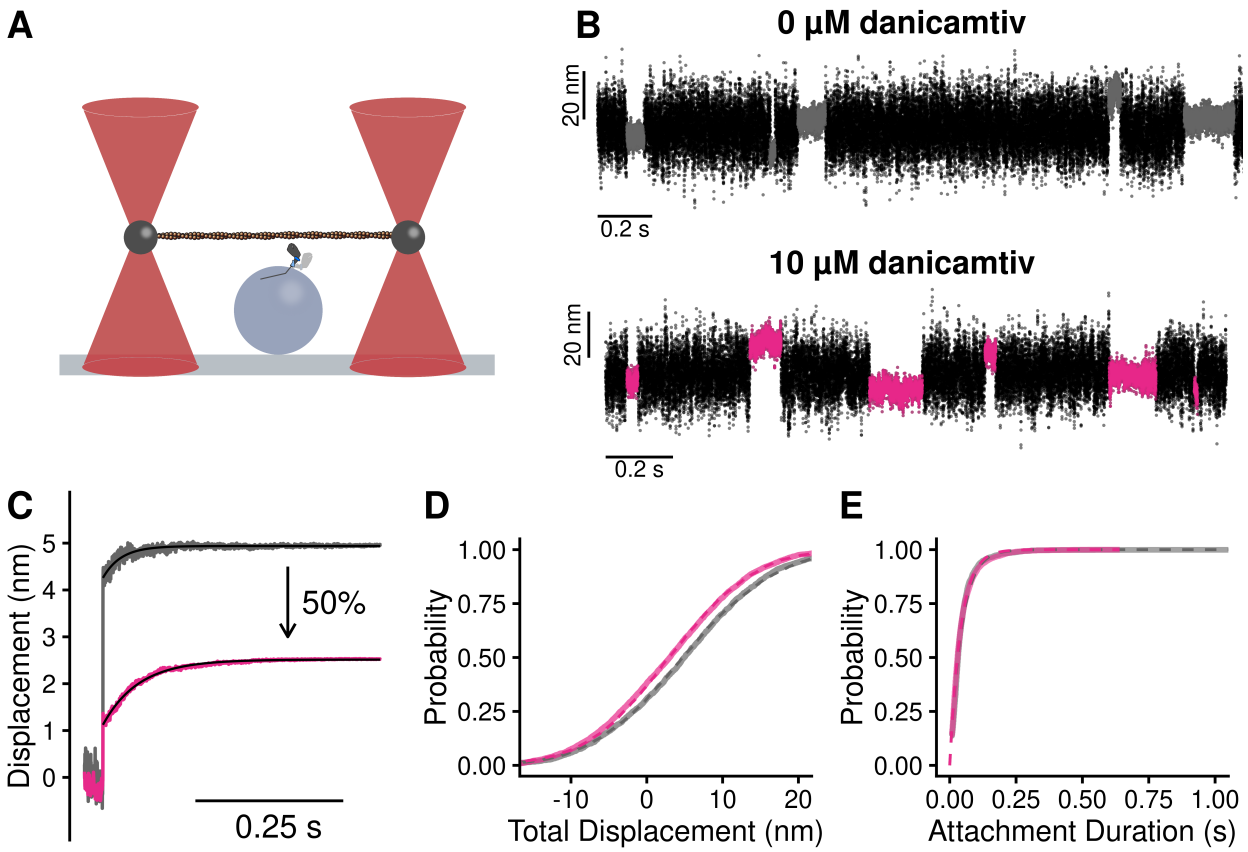
A
B
0 μM danicamtiv
20 nm
0.2 s
10 μM danicamtiv
20 nm
0.2 s
C
Displacement (nm)
50%
0.25 s
D
Probability
Total Displacement (nm)
E
Probability
Attachment Duration (s)

Figure 3

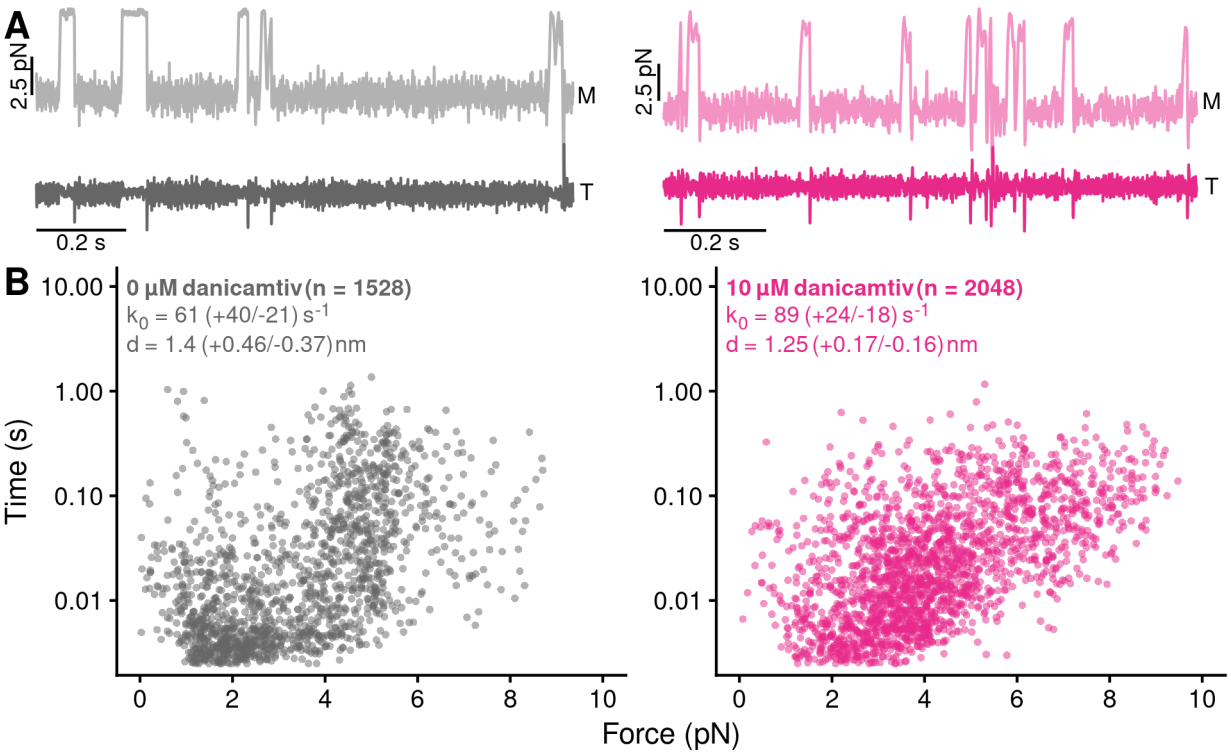
A
2.5 pN
M
T
0.2 s
2.5 pN
M
T
0.2 s
B
0 µM danicamtiv (n = 1528)
k0 = 61 (+40/-21) s-1
d = 1.4 (+0.46/-0.37) nm
10 µM danicamtiv (n = 2048)
k0 = 89 (+24/-18) s-1
d = 1.25 (+0.17/-0.16) nm
Time (s)
10.00
1.00
0.10
0.01
0
2
4
6
8
10
Force (pN)

Figure 4

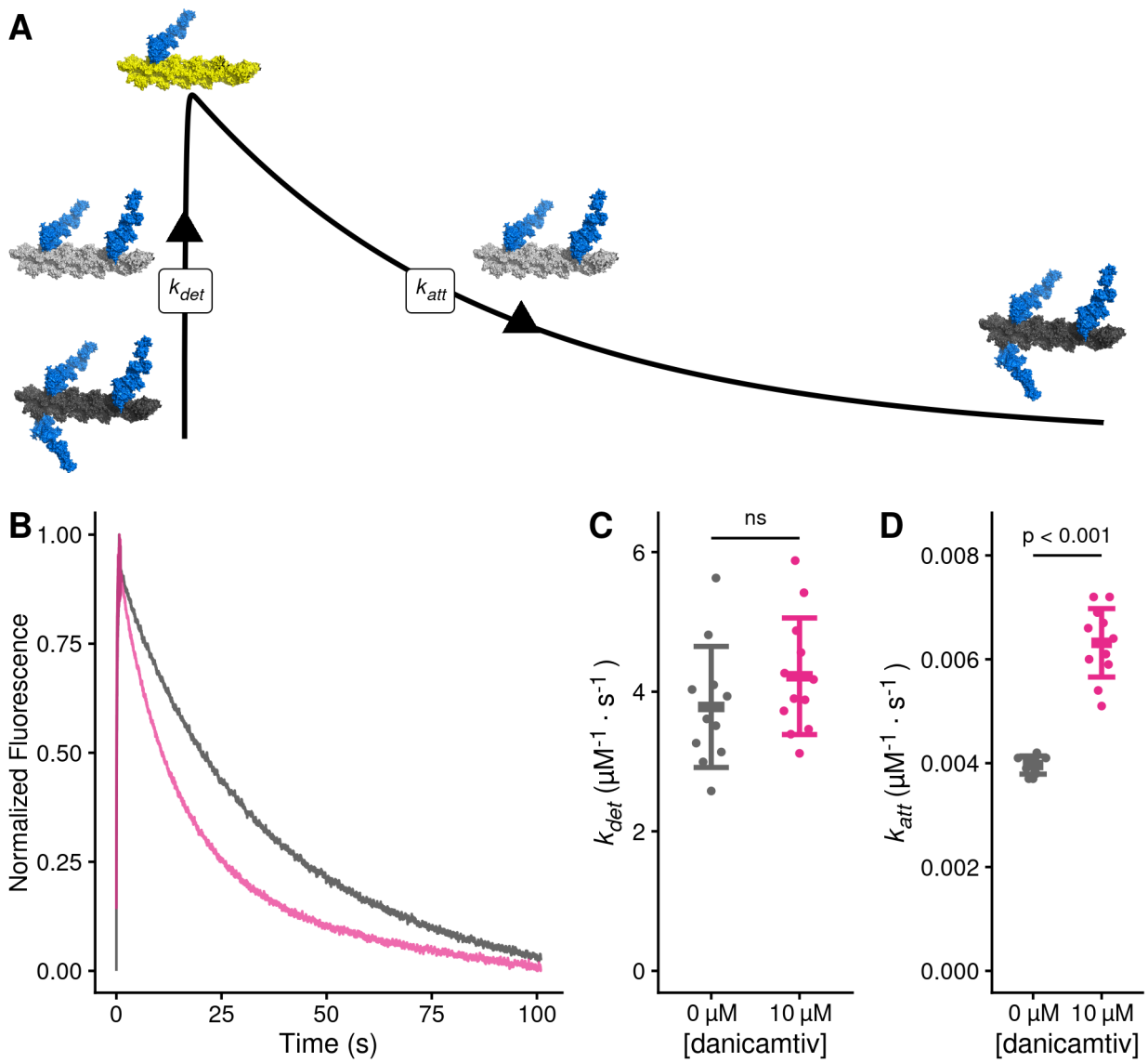
A
k_{det}
k_{att}
B
Normalized Fluorescence
1.00
0.75
0.50
0.25
0.00
0
25
50
75
100
Time (s)
C
ns
k_{det} (μM^{-1} · s^{-1})
6
4
2
0
0 μM
10 μM
[danicamtiv]
D
p < 0.001
k_{att} (μM^{-1} · s^{-1})
0.008
0.006
0.004
0.002
0.000
0 μM
10 μM
[danicamtiv]

Figure 5

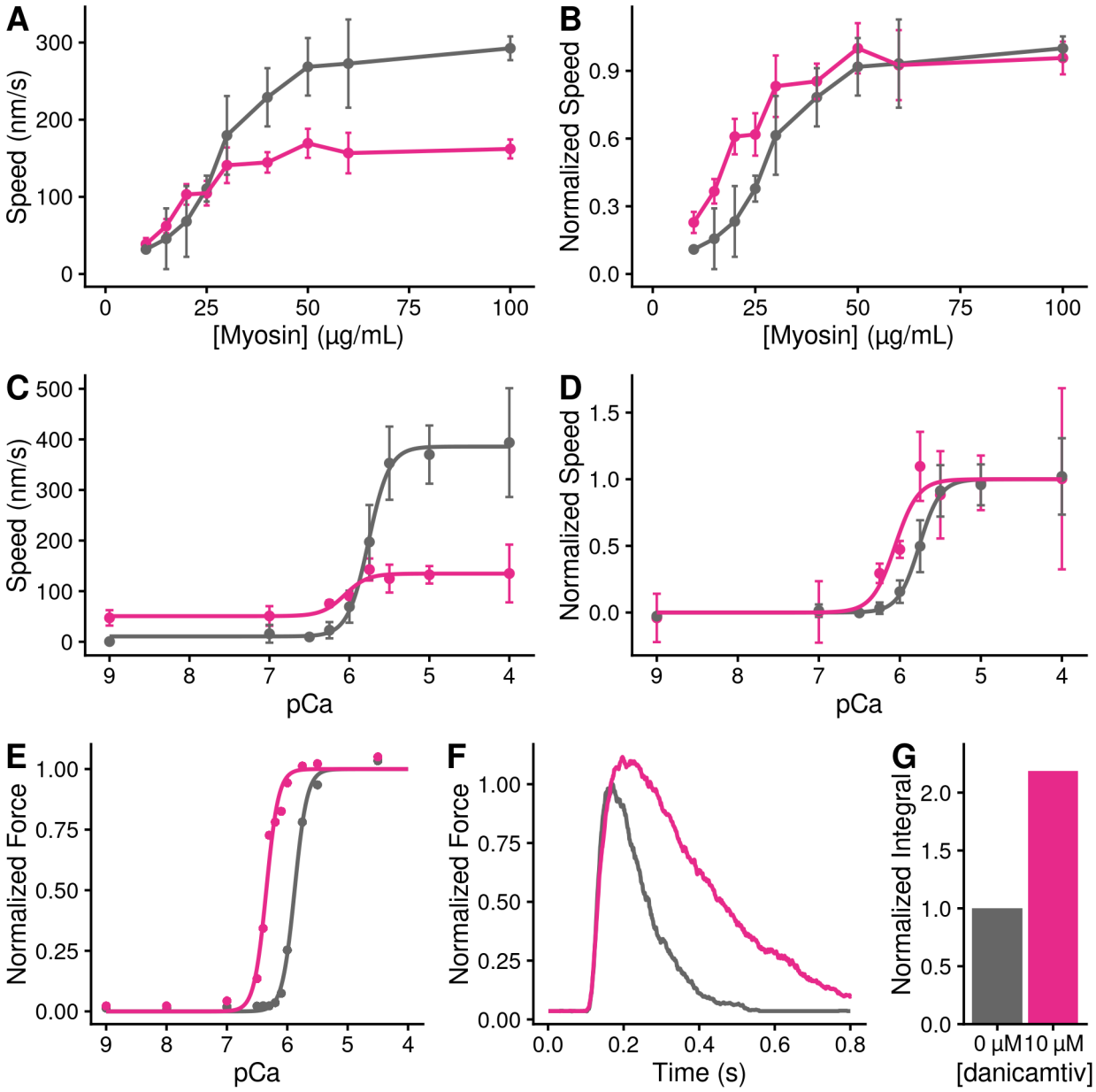
A
Speed (nm/s)
300
200
100
0
0
25
50
75
100
[Myosin] (µg/mL)
B
Normalized Speed
0.9
0.6
0.3
0.0
0
25
50
75
100
[Myosin] (µg/mL)
C
Speed (nm/s)
500
400
300
200
100
0
9
8
7
6
5
4
pCa
D
Normalized Speed
1.5
1.0
0.5
0.0
9
8
7
6
5
4
pCa
E
Normalized Force
1.00
0.75
0.50
0.25
0.00
9
8
7
6
5
4
pCa
F
Normalized Force
1.00
0.75
0.50
0.25
0.00
0.0
0.2
0.4
0.6
0.8
Time (s)
G
Normalized Integral
2.0
1.5
1.0
0.5
0.0
0 µM
10 µM
[danicamtiv]

Figure 6

627

Table 1. Solution kinetics summary.

Parameter	0 μM danicamtiv	10 μM danicamtiv	P-value
Steady State ATPase			
V_{max} (head^{-1}·s^{-1})	5.9 ± 0.4	7.0 ± 0.6	0.028
K_m (μM)	14.0 ± 2.5	8.1 ± 1.6	0.01
Catalytic Efficiency [V_{max}/K_m] (μM^{-1}·s^{-1})*	0.42 ± 0.08	0.86 ± 0.19	0.013
ATP Induced Dissociation			
$1/K_1'$ (μM)	269 ± 71	245 ± 38	0.64
k_{+2}' (s^{-1})	1054 ± 123	1053 ± 86	0.99
$K_1'\cdot k_{+2}'$ (μM^{-1}·s^{-1})*	4.0 ± 0.7	4.4 ± 1.1	0.64
ADP Release			
k_{+5}' (s^{-1})	73.2 ± 3.3	73.1 ± 3.3	0.96
k_{-5}' (μM^{-1}·s^{-1})*	4.1 ± 0.3	3.9 ± 0.2	0.40
K_5' (μM)	18.0 ± 4.6	18.6 ± 4.1	0.87
ATP Hydrolysis			
k_3 *(obs)* (s^{-1})	68.9 ± 20.8	63.7 ± 13.0	0.42
Single turnover assay			
k_{det} (μM^{-1}·s^{-1})	3.8 ± 0.9	4.2 ± 0.8	0.23
k_{att} (μM^{-1}·s^{-1})	0.0040 ± 0.0002	0.0063 ± 0.0007	< 0.001

*calculated value

628

629

Table 2. Optical trap summary.

Parameter	0 μM danicamtiv	10 μM danicamtiv	P-value
10 uM ATP			
Total Step (nm)	4.9 ± 9.7	3.0 ± 9.0	< 0.001
Total Step (nm)*	5.0	2.5	
k_f (s^{-1})*	51	26	
Detachment Rate (s^{-1})	23 (-2.5/+2.5)	24 (-0.8/+0.9)	0.39
Number of Events	2076	4776	
1 mM ATP			
Displacement (nm)	5.1 ± 6.8	2.6 ± 7.2	< 0.001
Detachment Rate (s^{-1})	41.4 (-6.6/+6.8)	34.2 (-5.7/+7.1)	0.15
Number of Events	965	1695	
Isometric Force Clamp			
k_0 (s^{-1})	61 (-21/+40)	89 (-18/+24)	0.12
d (nm)	1.40 (-0.37/+0.46)	1.25 (-0.16/+0.17)	0.35
Number of Events	1755	2107	

*ensemble average fit parameter

630

References

1. P. A. Heidenreich *et al.*, 2022 AHA/ACC/HFSA Guideline for the Management of Heart Failure: Executive Summary: A Report of the American College of Cardiology/American Heart Association Joint Committee on Clinical Practice Guidelines. *J Am Coll Cardiol* **79**, 1757-1780 (2022).
2. E. M. Hsich *et al.*, Heart Transplantation: An In-Depth Survival Analysis. *JACC Heart Fail* **8**, 557-568 (2020).
3. J. G. Rogers *et al.*, Chronic mechanical circulatory support for inotrope-dependent heart failure patients who are not transplant candidates: results of the INTrEPID Trial. *J Am Coll Cardiol* **50**, 741-747 (2007).
4. E. M. Green *et al.*, A small-molecule inhibitor of sarcomere contractility suppresses hypertrophic cardiomyopathy in mice. *Science* **351**, 617-621 (2016).
5. F. I. Malik *et al.*, Cardiac myosin activation: a potential therapeutic approach for systolic heart failure. *Science* **331**, 1439-1443 (2011).
6. B. P. Morgan *et al.*, Discovery of omecamtiv mecarbil the first, selective, small molecule activator of cardiac Myosin. *ACS Med Chem Lett* **1**, 472-477 (2010).
7. H. He *et al.*, Novel Small-Molecule Troponin Activator Increases Cardiac Contractile Function Without Negative Impact on Energetics. *Circ Heart Fail* **15**, e009195 (2022).
8. S. J. Lehman, C. Crocini, L. A. Leinwand, Targeting the sarcomere in inherited cardiomyopathies. *Nat Rev Cardiol* **19**, 353-363 (2022).
9. S. Shen, L. R. Sewanan, D. L. Jacoby, S. G. Campbell, Danicamtiv Enhances Systolic Function and Frank-Starling Behavior at Minimal Diastolic Cost in Engineered Human Myocardium. *J Am Heart Assoc* **10**, e020860 (2021).
10. J. R. Teerlink *et al.*, Cardiac Myosin Activation with Omecamtiv Mecarbil in Systolic Heart Failure. *N Engl J Med* **384**, 105-116 (2021).
11. A. A. Voors *et al.*, Effects of danicamtiv, a novel cardiac myosin activator, in heart failure with reduced ejection fraction: experimental data and clinical results from a phase 2a trial. *Eur J Heart Fail* **22**, 1649-1658 (2020).
12. P. O. Awinda, B. J. Vander Top, K. L. Turner, B. C. W. Tanner, Danicamtiv affected isometric force and cross-bridge kinetics similarly in skinned myocardial strips from male and female rats. *J Muscle Res Cell Motil* **45**, 115-122 (2024).
13. J. Choi, J. B. Holmes, K. S. Campbell, J. E. Stelzer, Effect of the Novel Myotrope Danicamtiv on Cross-Bridge Behavior in Human Myocardium. *J Am Heart Assoc* **12**, e030682 (2023).
14. K. B. Kooiker *et al.*, Danicamtiv Increases Myosin Recruitment and Alters Cross-Bridge Cycling in Cardiac Muscle. *Circ Res* **133**, 430-443 (2023).
15. M. S. Woody *et al.*, Positive cardiac inotrope omecamtiv mecarbil activates muscle despite suppressing the myosin working stroke. *Nat Commun* **9**, 3838 (2018).
16. S. R. Clippinger Schulte *et al.*, Single-molecule mechanics and kinetics of cardiac myosin interacting with regulated thin filaments. *Biophys J* **122**, 2544-2555 (2023).
17. C. Liu, M. Kawana, D. Song, K. M. Ruppel, J. A. Spudich, Controlling load-dependent kinetics of beta-cardiac myosin at the single-molecule level. *Nat Struct Mol Biol* **25**, 505-514 (2018).
18. S. J. Kron, J. A. Spudich, Fluorescent actin filaments move on myosin fixed to a glass surface. *Proc Natl Acad Sci U S A* **83**, 6272-6276 (1986).
19. J. A. Spudich, Hypertrophic and dilated cardiomyopathy: four decades of basic research on muscle lead to potential therapeutic approaches to these devastating genetic diseases. *Biophys J* **106**, 1236-1249 (2014).
20. S. K. Barrick, M. J. Greenberg, Cardiac myosin contraction and mechanotransduction in health and disease. *J Biol Chem* **297**, 101297 (2021).

21. E. M. De La Cruz, E. M. Ostap, Kinetic and equilibrium analysis of the myosin ATPase. *Methods Enzymol* **455**, 157-192 (2009).
22. S. R. Clippinger *et al.*, Disrupted mechanobiology links the molecular and cellular phenotypes in familial dilated cardiomyopathy. *Proc Natl Acad Sci U S A* **116**, 17831-17840 (2019).
23. J. C. Deacon, M. J. Bloemink, H. Rezavandi, M. A. Geeves, L. A. Leinwand, Identification of functional differences between recombinant human alpha and beta cardiac myosin motors. *Cell Mol Life Sci* **69**, 2261-2277 (2012).
24. T. Blackwell, W. T. Stump, S. R. Clippinger, M. J. Greenberg, Computational Tool for Ensemble Averaging of Single-Molecule Data. *Biophys J* **120**, 10-20 (2021).
25. J. T. Finer, R. M. Simmons, J. A. Spudich, Single myosin molecule mechanics: piconewton forces and nanometre steps. *Nature* **368**, 113-119 (1994).
26. M. J. Greenberg, H. Shuman, E. M. Ostap, Inherent force-dependent properties of beta-cardiac myosin contribute to the force-velocity relationship of cardiac muscle. *Biophys J* **107**, L41-L44 (2014).
27. M. J. Greenberg, H. Shuman, E. M. Ostap, Measuring the Kinetic and Mechanical Properties of Non-processive Myosins Using Optical Tweezers. *Methods Mol Biol* **1486**, 483-509 (2017).
28. T. Lin, M. J. Greenberg, J. R. Moore, E. M. Ostap, A hearing loss-associated myo1c mutation (R156W) decreases the myosin duty ratio and force sensitivity. *Biochemistry* **50**, 1831-1838 (2011).
29. T. Q. Uyeda, S. J. Kron, J. A. Spudich, Myosin step size. Estimation from slow sliding movement of actin over low densities of heavy meromyosin. *J Mol Biol* **214**, 699-710 (1990).
30. D. E. Harris, D. M. Warshaw, Smooth and skeletal muscle myosin both exhibit low duty cycles at zero load in vitro. *J Biol Chem* **268**, 14764-14768 (1993).
31. D. F. McKillop, M. A. Geeves, Regulation of the interaction between actin and myosin subfragment 1: evidence for three states of the thin filament. *Biophys J* **65**, 693-701 (1993).
32. D. M. Bers, Cardiac excitation-contraction coupling. *Nature* **415**, 198-205 (2002).
33. S. Kosta, D. Colli, Q. Ye, K. S. Campbell, FiberSim: A flexible open-source model of myofilament-level contraction. *Biophys J* **121**, 175-182 (2022).
34. S. Weiss, R. Rossi, M. A. Pellegrino, R. Bottinelli, M. A. Geeves, Differing ADP release rates from myosin heavy chain isoforms define the shortening velocity of skeletal muscle fibers. *J Biol Chem* **276**, 45902-45908 (2001).
35. A. P. Raduly *et al.*, The Novel Cardiac Myosin Activator Danicamtiv Improves Cardiac Systolic Function at the Expense of Diastolic Dysfunction In Vitro and In Vivo: Implications for Clinical Applications. *Int J Mol Sci* **24** (2022).
36. M. J. Greenberg, J. C. Tardiff, Complexity in genetic cardiomyopathies and new approaches for mechanism-based precision medicine. *J Gen Physiol* **153** (2021).
37. Y. Liu, H. D. White, B. Belknap, D. A. Winkelmann, E. Forgacs, Omecamtiv Mecarbil modulates the kinetic and motile properties of porcine beta-cardiac myosin. *Biochemistry* **54**, 1963-1975 (2015).
38. L. Greenberg *et al.*, Harnessing molecular mechanism for precision medicine in dilated cardiomyopathy caused by a mutation in troponin T. *bioRxiv* 10.1101/2024.04.05.588306 (2024).
39. S. R. Clippinger *et al.*, Mechanical dysfunction of the sarcomere induced by a pathogenic mutation in troponin T drives cellular adaptation. *J Gen Physiol* **153** (2021).
40. S. K. Barrick, L. Greenberg, M. J. Greenberg, A troponin T variant linked with pediatric dilated cardiomyopathy reduces the coupling of thin filament activation to myosin and calcium binding. *Mol Biol Cell* **32**, 1677-1689 (2021).